A hybrid reconstructed discontinuous Galerkin method for incompressible flows on arbitrary grids

***Fan Zhang[1], Jian Cheng[2], and †Tiegang Liu[1]**

[1]School of Mathematics and System Science, Beihang University, China
[2]Laboratory of Computational Physics, Institute of Applied Physics and Computational Mathematics, China

*Presenting author: zhangfan1990@buaa.edu.cn
†Corresponding author: liutg@buaa.edu.cn

Abstract

The discontinuous Galerkin (DG) methods have attained increasing popularity for solving the incompressible Navier-Stokes (INS) equations in recent years. However, the DG methods have their own weakness due to the high computational costs and storage requirements. In order to tackle this problem, in this paper, a hybrid least-squares reconstruction DG (rDG) method, namely P_1P_2(HLSr), is presented to obtain a quadratic polynomial solution from the underlying linear DG solution by use of a hybrid recovery and reconstruction strategy. This hybrid rDG method combines the simplicity of the reconstruction-based DG method and the accuracy of the recovery-based DG method, and has the desired property of 2-exactness which is violated by the original least-squares rDG method. The inviscid term of the INS equations, which is split into the nonlinear convective term and the linear Stokes operator, is discretized by using a simplified artificial compressibility flux. More specially, the nonlinear convective term is discretized in divergency form by using the local Lax-Friedrichs flux, while the Stokes operator is discretized by using the artificial compressibility flux which is provided by the exact solution of a Riemann problem associated with a local artificial compressibility perturbation of the Stokes system. The discretization of the viscous term follows the simple direct DG (DDG) method. A number of incompressible flow problems, in both steady and unsteady forms, for a variety flow conditions are computed to numerically assess the spatial order of convergence of the P_1P_2(HLSr) method, which demonstrate its ability to achieve the designed optimal 3rd-order of accuracy at a significantly reduced computational costs.

Keywords: Incompressible Navier-Stokes equations, reconstructed methods, discontinuous Galerkin method, artificial compressibility, arbitrary grids

Numerical results

Kovasznay problem

The analytic solution for the 2D INS equations was derived by Kovasznay. The analytical expression for the velocity and the pressure is

$$u(x,y) = 1 - e^{\lambda x}\cos(2\pi y),$$

$$v(x,y) = \frac{\lambda}{2\pi}e^{\lambda x}\sin(2\pi y),$$

$$p(x,y) = -\frac{1}{2}e^{\lambda x}.$$

Here, $\lambda = \frac{Re}{2} - \sqrt{\frac{Re^2}{4} + 4\pi^2}$. The computational domain is $\Omega = (-\frac{1}{2}, \frac{3}{2}) \times (0, 2)$ with prescribed Dirichlet boundary conditions on $\partial\Omega$. The Reynolds number is Re=10 and the artificial compressibility parameter is c^2=1.0.

The comparisons among the numerical results obtained by the DG(P_1), DG(P_2) and P_1P_2(HLSr) methods are presented in Tab.1. It can be seen that the P_1P_2(HLSr) method, as expected, adding one order of accuracy to the underlying DG(P_1) method and even having higher order of accuracy for the pressure than the DG(P_2) method. Although the DG(P_2) method does yield a slightly more accurate solution than the P_1P_2(HLSr) method at the same grid resolution, however, it is obtained at the cost of more number of the degrees of freedom which leads to a dramatic increase of the computational cost. The detailed convergence history, which contains the number of iteration steps and the CPU time (s) to reduce the residual by 8 orders of magnitude are presented in Tab.2.

Tab1. Convergence results for the Kovasznay problem.

Grid size	No. DOFs	$\|e_{\mathbf{u}}\|_2$		$\|e_p\|_2$		$\|e_{\nabla\cdot\mathbf{u}}\|_2$	
		Error	Order	Error	Order	Error	Order
DG(P_1)							
8×8	192	3.19e-1		5.02e-1		1.41e-0	
16×16	768	7.89e-2	2.02	1.25e-1	2.01	6.86e-1	1.04
32×32	3,072	1.92e-2	2.04	3.42e-2	1.87	2.40e-1	1.52
64×64	12,288	4.56e-3	2.07	9.92e-3	1.79	7.00e-2	1.78
DG(P_2)							
8×8	384	6.00e-2		6.29e-2		4.48e-1	
16×16	1536	7.35e-3	3.03	1.18e-2	2.41	9.25e-2	2.25
32×32	6,144	9.21e-4	3.00	2.37e-3	2.32	1.95e-2	2.25
64×64	24,576	1.26e-4	2.87	5.15e-4	2.20	4.40e-3	2.15
P_1P_2(HLSr)							
8×8	192	1.39e-1		2.84e-1		8.65e-1	
16×16	768	1.71e-2	3.02	4.29e-2	2.73	2.00e-1	2.11
32×32	3,072	2.08e-3	3.04	6.63e-3	2.77	3.48e-2	2.57
64×64	12,288	2.24e-4	3.22	1.02e-3	2.70	5.49e-3	2.66

Tab.2 Convergence history for the Kovasznay problem.

Grid size	Iteration step			CPU time (s)		
	DG(P_1)	DG(P_2)	P_1P_2(HLSr)	DG(P_1)	DG(P_2)	P_1P_2(HLSr)
8×8	95	95	93	9.65	28.08	3.63
16×16	127	126	126	23.71	103.13	12.25
32×32	159	204	156	84.40	557.36	84.91
64×64	201	250	190	679.12	5289.36	785.05

Lid-driven cavity flow

The lid-driven cavity flow has been widely used as a validation case for numerical method of the INS equations. The problem has simple geometry and boundary conditions. The standard

case is fluid contained in a square domain $\Omega = (0,1)^2$ with homogeneous Dirichlet boundary conditions on all sides except on the upper side where the velocity is prescribed as $\mathbf{u} = (1,0)$. Here, we compare the performances of the DG(P_1), DG(P_2) and P_1P_2(HLSr)methods at high Reynolds number by the lid-driven cavity flow problem with Re=1,000, 5,000 and 10,000.

The u-velocity and pressure profiles along a vertical line and the v-velocity and pressure profiles along a horizontal line passing through the geometric center of the cavity respectively are presented in Fig.1-Fig.3. It can be seen that the present method is able to mimic the available results with great accuracy, the profiles are in good agreement of the reference results.

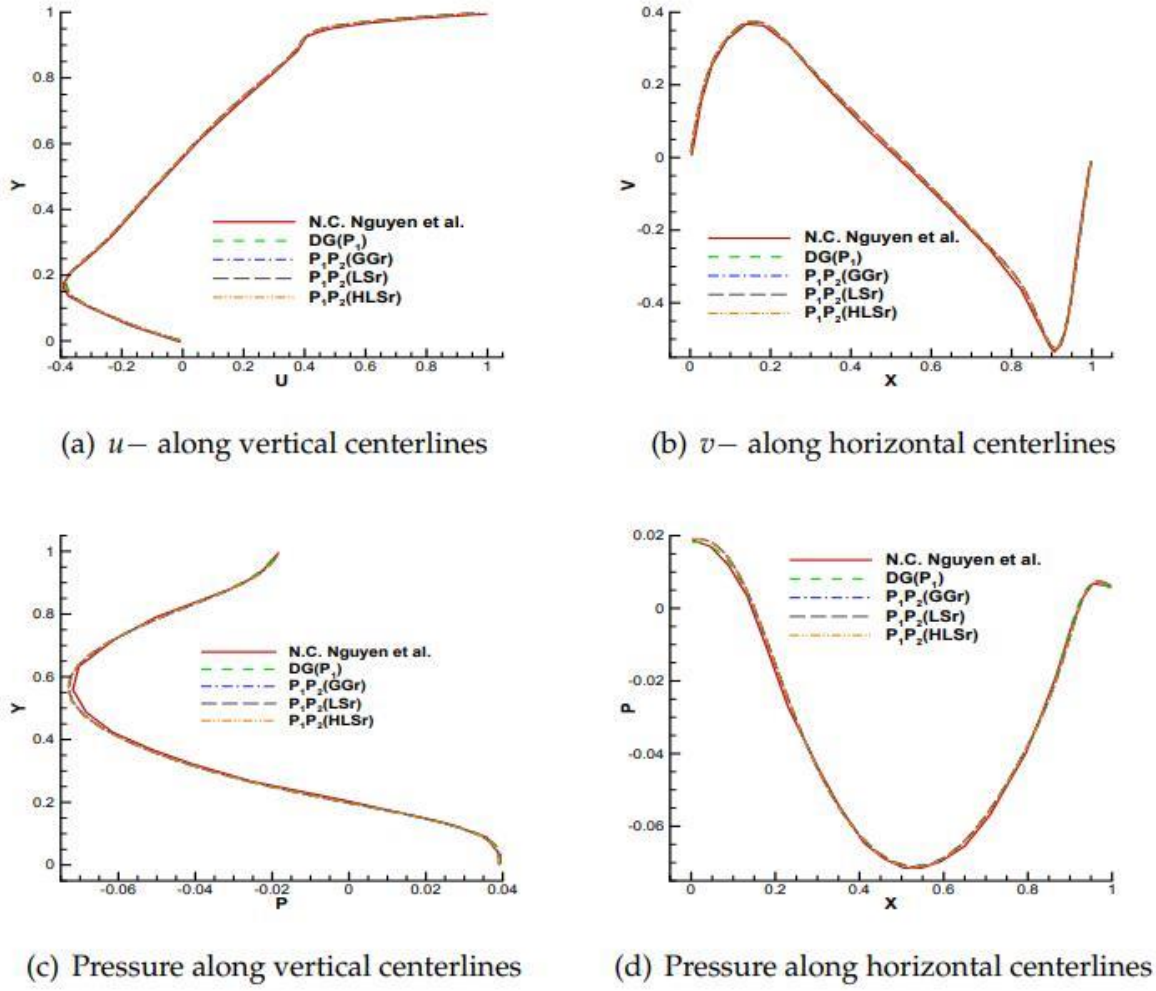

(a) $u-$ along vertical centerlines

(b) $v-$ along horizontal centerlines

(c) Pressure along vertical centerlines

(d) Pressure along horizontal centerlines

Fig.1 Results for the lid-driven cavity flow at Re=1,000.

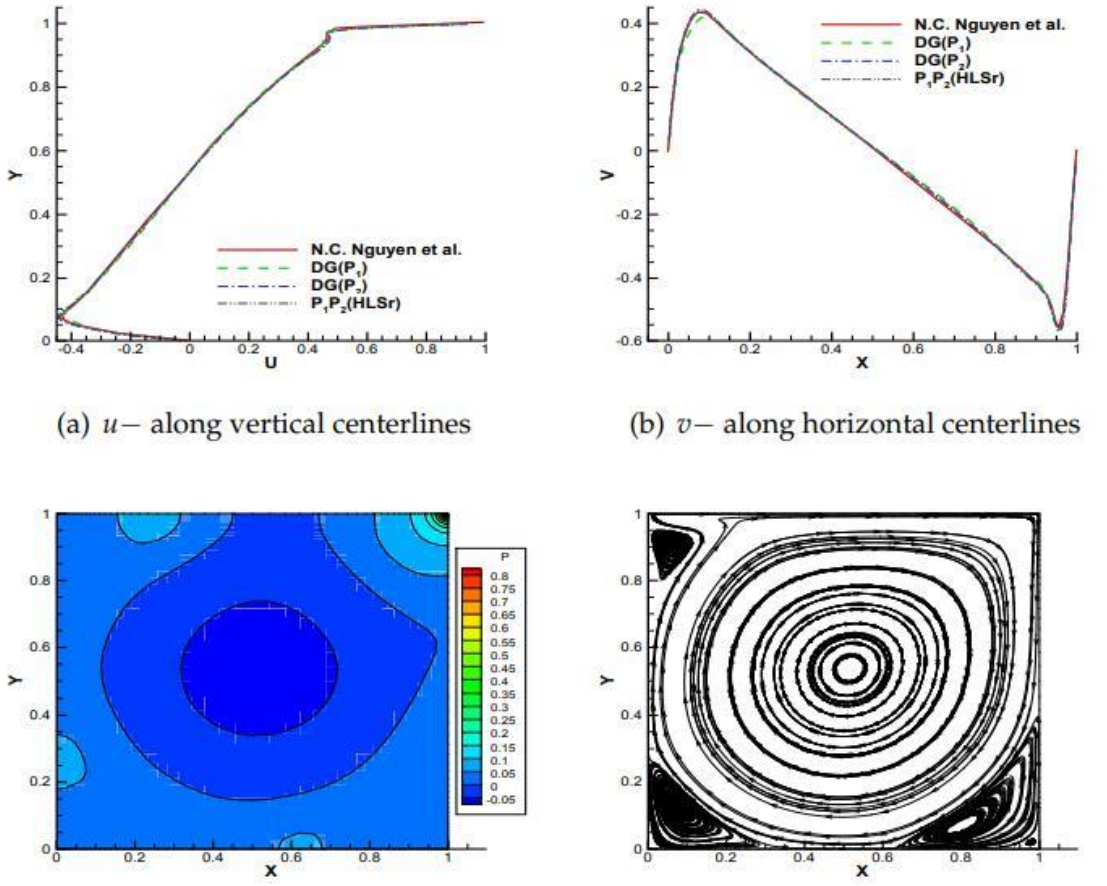

(a) $u-$ along vertical centerlines

(b) $v-$ along horizontal centerlines

(c) Pressure of P_1P_2(HLSr) solution

(d) Streamlines of P_1P_2(HLSr) solution

Fig.2 Results for the lid-driven cavity flow at Re=5,000.

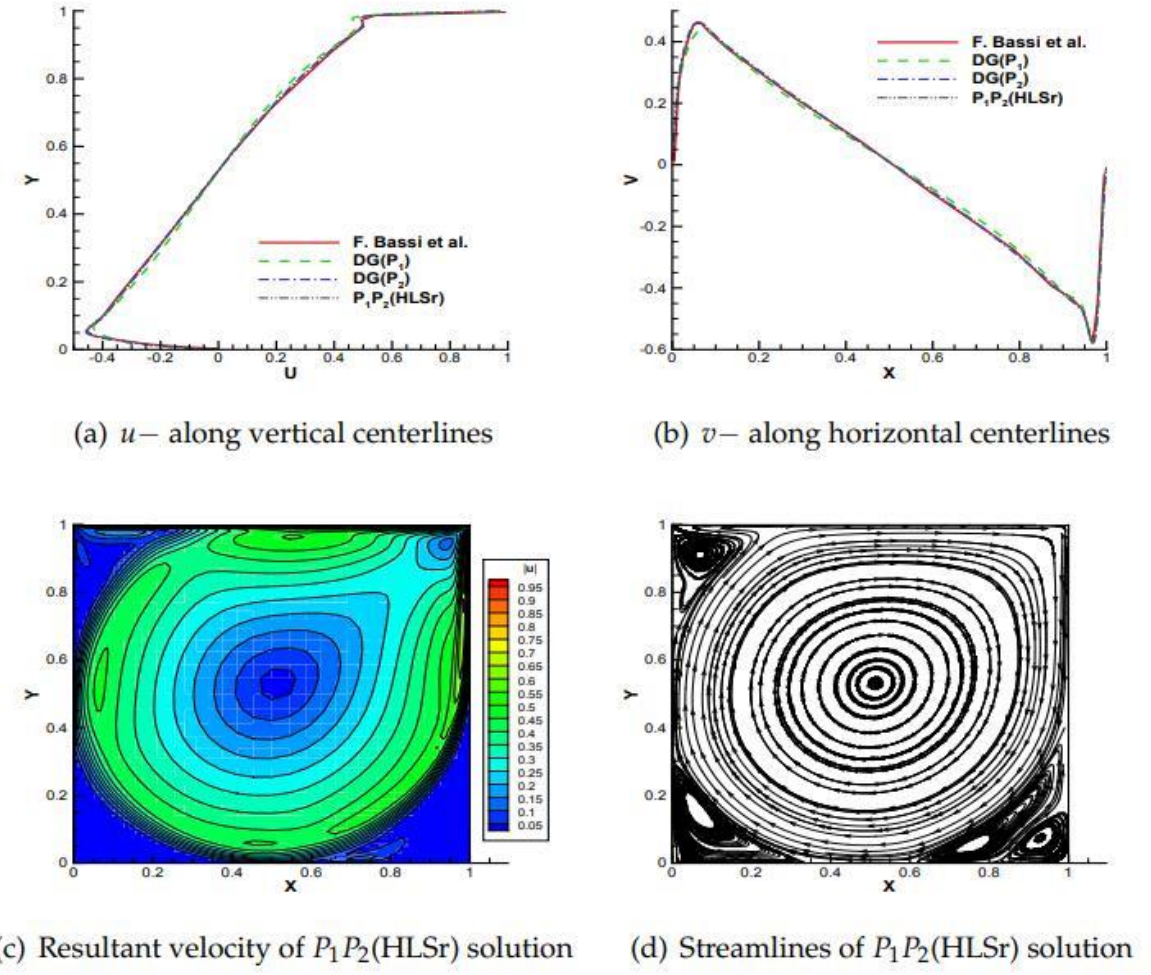

(a) $u-$ along vertical centerlines

(b) $v-$ along horizontal centerlines

(c) Resultant velocity of P_1P_2(HLSr) solution

(d) Streamlines of P_1P_2(HLSr) solution

Fig.3 Results for the lid-driven cavity flow at Re=10,000.

Steady flow over a circular cylinder

A flow past a circular cylinder at a Reynolds number of 20 and 40 respectively based on a uniform free-stream velocity $\mathbf{u} = (1, 0)$ with no-slip boundary conditions on the cylinder surface is considered in this case. At both of these two Reynolds numbers, the flows are laminar and steady and were studied quite extensively in both measurements and numerical calculations.

Fig.4 shows the streamlines and the vortex behind the cylinder computed by the P_1P_2(HLSr) method at Re = 20 and Re = 40, respectively. It is clear to see that a pair of stationary recirculating regions appears in the wake of the cylinder for each condition and the length of the recirculating region increases with the Reynolds number.

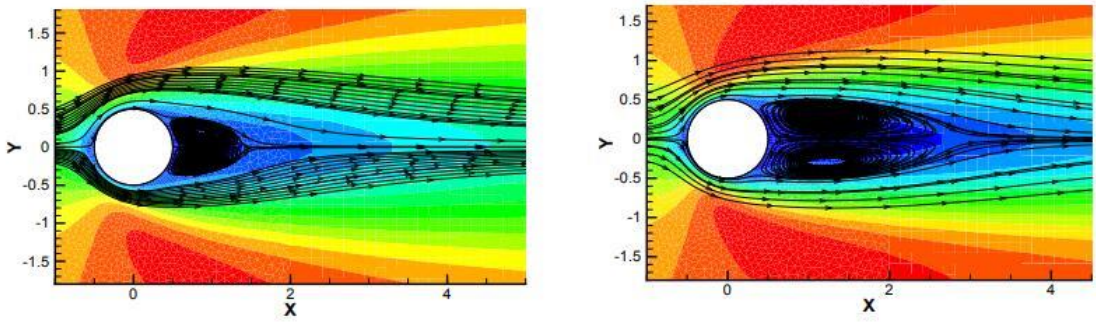

(a) $Re=20$ (b) $Re=40$

Fig.4 Streamlines plot of steady flow past around a circular cylinder based on P_1P_2(HLSr).

Next, we calculate the friction and pressure drag coefficients, the total drag coefficients, the front and rear stagnation pressure coefficients, and recirculation lengths obtained for the steady flows at Re=20 and 40, respectively. The results are summarized in Tab.3.

Tab.3 Comparison of results for steady flow past a circular cylinder.

Source	C_{DF}	C_{DP}	C_D	$C_p(0)$	$-C_p(\pi)$	L_w/D
$Re=20$						
R.P. Bharti et al.	0.8211	1.2244	2.0455	1.2889	0.5457	0.9164
DG(P_1)	0.7882	1.2241	2.0132	1.2918	0.5505	0.9301
DG(P_2)	0.8078	1.2257	2.0336	1.2956	0.5492	0.9051
P_1P_2(HLSr)	0.8074	1.2256	2.0330	1.2943	0.5496	0.9051
$Re=40$						
R.P. Bharti et al.	0.5316	0.9976	1.5292	1.1636	0.4798	2.2252
DG(P_1)	0.5072	0.9959	1.5031	1.1649	0.4821	2.0507
DG(P_2)	0.5234	0.9961	1.5196	1.1674	0.4804	2.1233
P_1P_2(HLSr)	0.5232	0.9962	1.5195	1.1663	0.4810	2.2685

An excellent correspondence can be seen to exist between the present and literature results which demonstrate that our method can provide an attractive alternative for solving the INS equations on arbitrary grids.